17th ICAS Congress - Stockholm, 9th-14th September 1990
Paper No. 90-2.7.1

AERODYNAMIC DESIGN FOR A NEW REGIONAL AIRCRAFT

Dr. E. Greff *

Deutsche Airbus GmbH, Bremen, F.R.G. +

Abstract

Changing airways szenarios and aggravated congestion led to a surge of orders for new regional aircraft which will cover increased range and passenger capacity than todays commuter aircraft. MPC 75 is designed to fill in the gap around 80 to 120 passengers with a typical range of 1300 nm. A feasibility study and detailed design work on different new technologies as the natural laminar flow wing (NLF), turbulence management by riblet films and propfan propulsion was performed. Supported by research work on a flying test-bed and corresponding windtunnel tests a first NLF-wing was designed and validated in competition to a modern transonic wing with turbulent flow. The integration aspects of a propfan propulsion were addressed by means of CFD methods and will be checked by experiment later on.

A trade-off analysis using DOC-methods shows only minor advantages at current fuel prices and hence a conventional configuration with wing-mounted turbofans was selected for further optimization. An all-new design of that kind should surpass current regional aircraft and derivatives also and requires much less effort in terms of non-recurring costs.

I. Introduction

The advent of deregulation in the USA, the liberalization in Europe and the burgeoning of the hub-and-spoke system led to a surge of orders for smaller aircraft and this is continuing. Assuming a world average growth rate of 5.1% the in-house annual market forecast from 1989 to 2008 predicts a demand of 11150 new aircraft being worth a business of 570 billion $ (1989). 60% of this market is single aisle with 80% replacement of older aircraft and 20% growth share. This is in good agreement with ICAO predictions[1]. After recovery from the world wide depression in the beginning of the 80's the rush to buy new aircraft has created for manufacturers the longest backlog in history.

The airport and airways situation however poses major constraints on the huge fleet expansion. As a consequence of deregulation airlines merged and developped the hub-and-spoke system which led to a significant increase in traffic delays over the congested hubs. According AEA more than 25% of all flights were delayed in 1988 by more than 15 minutes and this is increasing. Following European airline officials[2] in that year the unproductive flight hours summed up to DM 500 million.

Congestion affects growth and hence the fleet expansion can be realized only when the system is restructured in order to overcome the constraints. As only few new airports are being built in the vicinity of major hubs a possible szenario (Fig. 1) is the switch from hub-spoke service to hub-by-passing service, i.e. more point-to point services with smaller aircraft. Especially the regional market is facing a complete restructuring and the big airlines are getting more and more interested in completing their fleet with single aisle aircraft for this purpose. Generally the regional airliner of the 1990's will have to serve longer routes up to 2000 nm with increased passenger capacity (75-130) than its predecessors. Due to the limited availability of runway length on regional airports it should have a very good field performance or even STOL-capability.

On the lower ranges an increased competition with high-speed rail systems as to mention magnetic levitation trains will replace some uneconomic short range flights whereas on the upper range an increasing demand for feeder service to the new kind of airport currently discussed to ease the congestion - the wayport [3,4] which is a huge transfer airport in a remote area for the large intercontinental services with hyperjumbos, or new high-speed civil transports (HSCT) - is forecasted.

New technologies and improvements in air traffic control procedures could increase the airspace capacity by 30% but will reduce horizontal and vertical separation thus resulting in a more unified cruise speed and more complicated manoeuvring for ascent and descent avoiding the traditional long ILS glide path.

Taking into account all the driving forces to possible market changes a market potential of 4650 new regional aircraft (65-150 pax) is predicted (Fig. 2) where 45% are located in USA and 20% are concentrated on Europe as well as Far East. The competitors in this market segment are derivatives as to mention the BAe 146-300, the MD90 series, the Fokker 100 and the B737-500 whereas new aircraft in the range of 75 to 120 seats will not be available in the mid 90's. MPC 75 is developped to fill in this gap with a possible share of ~45% and entry-into-service in 1995.

The economical success of an all-new regional aircraft highly depends upon its fuel efficiency in terms of specific range, its comfort and its operational flexibility. In the situation of low fuel prices and short ranges (the most probable range for a regional jet with 1300 nm design mis-

* Head of Aerodynamic Design Department
+ Former MBB-UT, Transport Aircraft Group

sion is about 400-500 nm) the cost of ownership is predominant and the fuel share is in the order of 10% only. Hence especially for these aircraft a more deliberate trade-off analysis of new technologies has to be done than it is the case with wide-body aircraft[5], where fuel efficiency is more profitable for the airlines.

The set of requirements for the baseline aircraft (Fig. 3) is subject to change within a changing szenario. Hence we see a compelling need to offer a design with high operational flexibility. The most stringent requirement is the field length requiring a very effective high lift system. Due to the possible change in ACT and the drive to a higher unified cruise Machnuber a sufficient Machnumber flexibility up to MMO = 0.8 is requested. The wing area is more or less defined by field requirements and single engine ceiling. This results in very low wing loadings for cruise with typical lift coefficients in the order of 0.3 to 0.4 for the baseline aircraft. Modern transonic wings however usually have their L/D-optimum at lifts of CL = 0.5 to 0.55, i.e. such a wing would be operated in extreme off-design cases with corresponding high performance offsets. Hence it is a challenge for the designer to drive the optimum to sufficient low lifts without substantial losses in buffet boundary as this would penalize the ultimate stretch version.

In the following this paper will focus on the status of aerodynamic design work for MPC 75 and the trade-offs already performed for the basic aerodynamic technologies natural laminar flow/ variable camber vs. a conventional turbulent transonic wing and turbulence management via riblets. Design integration aspects of the propulsion system for a propfan are discussed as well as for a wing-mounted high by-pass turbofan. In the beginning of the predevelopment phase no turbofan in the required thrust range was available, but the szene is changing and even in the utmost lower passenger class of the 40-50 seaters new turbofans are emerging[6]. In the meantime MPC 75 has gone through a major reconfiguration[7] as the trade-offs have shown that a propfan propulsion would not sell off at fuel prices below 1,5 $ and the availability for a new turbofan in the required thrust range 12100 to 16000 Lbs (Take-off, sea level static) becomes most probable.

II. Basic Technologies and their Configurational Aspects

The original design of the potential competitors for MPC 75 dates back to 1975 and even before whereas the Fo100 wing was changed significantly with all the problems inherent in the modification of an existing wing geometry by means of leading edge (L.E.), trailing edge (T.E.) and tip extensions. E. Obert[8] reported that 12 wing geometries were tested and 1928 windtunnel hours were consumed - an effort which is comparable to a complete new design.

The transport aircraft group MBB-UT (after the recent merger Deutsche Airbus GmbH) gained experience in continous design work for the complete configuration in high and low speed in the Airbus Program from the very beginning over the past 15 years. The achievements in aerodynamic performance improvement from the late A300 to the A330/A340 are outstanding (more than 30% L/D increase without size-effect). The application of the latest state-of-the-art to the design of a regional airliner would already give an all-new design which could surpass existing derivative aircraft. Hence the trade-off is done by using a comparison of an all-new turbofan aircraft with A320 technology and a more advanced design using different new technology items.

Despite the fact, that the achieved standard is already high the field of aerodynamics is still offering a high potential for further fuel savings which is quoted to be ~ 20 to 30% due to laminarization and turbulence management. This however would require rather complex suction devices which would be probably feasible for a long range aircraft and not for a regional aircraft. A passive laminarization however by means of airfoil shape seemed less complex and feasible for the moderate Reynoldsnumbers of such an aircraft.

Besides the aerodynamics most promising gains were seen in the new propulsion systems emerging and the use of composites for primary strucutre namely the wing box thus allowing a further increase in aspect ratio[9,10].

2.1 Configurational Aspects

The corresponding general arrangements for the different baseline aircraft are compared in Fig. 4. The main differences illustrated here are in the engine position, wing planform and high-lift system. A more detailed discussion of the configurational aspects is given in[10].

For UDF-propulsion a rear-end mounting turned out to be the only practical solution with all the negative aspects on weight, c.g. travel, tail size, stability and control already known from rear-mounted turbofans but even more enhanced. The NLF-wing takes advantage of this configuration as a wing mounted engine would considerably reduce laminar flow runs due to engine noise.

The achievable Machnumber with the UDF is quite moderate (Mcruise = 0.7 - 0.75), which allows lesser wing sweep (17° at the leading edge) which is beneficial with respect to the cross-flow instability and attachment-line contamination. This results in a wing planform with hardly a planform crank which gave rise to an in-depth investigation into the possibility of a trapezoidal wing with its clear aerodynamic advantages of a near elliptic load distribution and the possibility to gain maximum lift through an unsegmented constant chord (30%) flap together with a fuselage mounted main landing gear (MLG). This MLG however is of an articulated type and would be rather complex and expensive as a spare part so that the possible gain was outbalanced.

The required surface quality for longer laminar flow runs (see chapter 5) can only be achieved with an integrated CFRP nose thus prohibiting the installation of L.E.-devices as slats or Krüger flaps. The high by-pass ratio of the UDF has the negative effect that the bleed air extractions are accompanied by drastic thrust reductions. Hence an anti-icing system using hot air was ruled out by the engine. In combination with the NLF wing and

the integrated CFRP-Nose a liquid anti-icing and cleaning system was the adequate solution. This dual function is necessary for the NLF wing in order to prevent substantial loss of laminar flow due to insect contamination. Operational tests of such a system were foreseen.

The turbofan-alternative may have higher wing sweep in order to attain more speed flexibility. It may also have L.E.-devices which would allow to optimize the wing area closer to the cruise requirement provided the stretch potential and fuel volume is still sufficient with a smaller wing.

2.2 Potential of NLF

The drag breakdown in cruise condition for a typical narrow-body transport aircraft using a modern transonic wing is given in Fig. 5. It clearly shows that the friction drag is the major component which can be reduced by more than 50% using Laminar Flow Control (LFC) or Hybrid Laminar Flow Control (HLFC). The more moderate NLF concept would still allow an overall improvement in L/D in the order of 10%. Combined with an increased aspect ratio from 9.4 to 11 a 15% gain in L/D-optimum with respect to A320 technology seems achievable. However the realization for swept wings of transonic transports is very difficult and subject to several constraints. In Fig. 6 the relationship between wing sweep, Reynolds number and L.E. radius is shown. Natural laminarized flow (NLF) by shaping the airfoils is confined to the region left of the boundary whereas LFC is the only chance for Airbus category aircraft. The regional aircraft design seems feasible without active laminarization.

Since the 1930's aerodynamic research was devoted to laminar flow especially to LFC and HLFC as it was thought that NLF was not feasible due to surface quality. NASA's halfbillion dollar program ACEE which began in 1976 revived the efforts in LFC significantly [11,12,13] and let to outstanding in-flight experiments with several prototype applications with no application in service so far. Todays manufacturing tolerances and new materials however have already decreased the parasitic drag level to ~ 3% aircraft drag while it used to be twice this value 15 years ago. With these tolerances laminar flow runs of more than 50% chord seem feasible and in 1986 a national research program devoted to the NLF wing was started as a joint effort of industry and research institutes. A summary of the german view on laminarization and the status is given in [14,15].

In comparison to a conventional transonic airfoil the typical NLF design is depicted in Fig. 7. The aim is to achieve a pressure distribution with accelerated flow regions and corresponding laminar flow extent. The figure already points out the problem of significant higher recompression gradients towards the T.E. A careful analysis of different recompression types, i.e. degressive (Stratford) or progressive, and the magnitude of rear loading must be carried out in order to avoid separation. Especially at higher Machnumbers the shock-wave boundary-layer interaction may offset the gain in friction drag and off-design cases with fully turbulent flow should be feasible without significant separations and lift losses thus evoking unfavourable handling characteristics.

The profile drag reduction may be in the order of > 50% with laminar flow runs of 60% chord. This extent may be achievable for 80% of the exposed area whereas inboard the influence of the wing-body juncture causes a turbulent wedge of some percent span. With a wing contribution of nearly 40% of the total aircraft friction and pressure drag this would save some 10% of aircraft cruise drag at the design cruise Machnumber. In off-design conditions laminarization effects tend to reduce due to either pronounced suction peaks at lower Machnumber and corresponding Tollmien-Schlichting instability (TSI) or significant wave drag increase at higher Machnumbers. This adverse effect must be avoided and a comprehensive tool for this purpose is available with the Variable Camber (VC) whose effect on the laminar bucket is also shown in Fig. 7. This leads to the concept of the intelligent wing [16] with VC integrated in an automated control system. The benefits and design integration aspects of VC on conventional transports were already studied in detail [17] and must be transferred to the NLF airfoil type.

2.3 Turbulence Management (Riblets)

Another way of boundary layer control is possible due to a reduction of turbulent friction drag by manipulation of the turbulence structure within the turbulent boundary layer. So-called riblets suppress vortex formations near the wall. A potential of 8% friction drag reduction is envisaged from experiments on flat plates . The structure of these films is very fine, only about 0.05 mm between two ridges (Fig. 8). The realization problems are more in the operational area, for instance the application on the surface, the cleaning, the tensile strength and degradation due to environmental effects or agressive fluids like skydrol. A 2% overall drag improvement was estimated for this configuration so far which has to be verified. In a technology working group within the Airbus partners a flight test on an A320 was performed recently which supports this target value and additionally a long term test with a Lufthansa A300-600 was conducted to check the operational aspects. Generally the method is feasible and it is a question of trade-off analysis, manufacturing and maintenance now whether this technique will be applied or not. Hence this subject is not dealt with in further detail in this paper.

2.4 Integration of Advanced Propulsion Systems

The energy crisis in the late 70's has set off a considerable effort in the engine industry which were concentrated on either turbofans with very high by-pass ratio (superfan) or the open rotor concept called propfan or unducted fan (UDF). The common key to better SFC is driving the by-pass ratio to extreme values and thus increasing the propulsive efficiency while maintaining the cruise speed of current turbofans. The open rotor promised 25% to 40% less SFC depending on the reference turbofan (Fig. 9). But even in the case of a common core of latest technology propfans still offered 20% to 25% fuel savings which gave rise to considerable efforts amongst almost all airframe manufacturers in the world and several demonstrators were flown in the last years. Initial enthu-

siasm declined however after a thorough study of the configurational repercussions [10] counteracting the uninstalled fuel burn advantage.

Projects like the MD-91 UHB and the B7-J-7 were discarded and MDC now offers the MD-91/92V family with V2500 turbofans. The common message is that only at fuel prices exceeding 1,5 $ this technology would sell off and also MPC 75 was reconfigured to a turbofan propelled version in the midth of 1989 [6,7]. However the research work originally devoted to MPC 75 was continued in the sense of a technology readiness program and some intermediate results are reported in chapter VI.

III. Aerodynamic Development Concept

The aerodynamic design of a transport aircraft with transonic wings requires extensive configuration iterations through repeated windtunnel test loops. CFD methods are becoming more important in the predevelopment phase in order to limit the number of iterations and by means of a combination of windtunnel testing and efficient direct-inverse methods the design can be optimized [18].

The continuous development of transonic wings for the Airbus family has led to a well established procedure which guarantees a performance prediction of high confidence level. For the development of a configuration with wing-mounted turbofans and a conventional transonic wing in general 3 types of models are necessary which are shown in Fig. 10.

1. A 1:18 scale complete model tested in the High Speed Tunnel of ARA in Bedford. This model, due to its modular structure, is used for HS-wing development steps and performance predictions. Later on in the design phase the support will be changed to a twin sting support in order to determine the sting interference and to develop the rear fuselage/tail unit.

2. A 1:10 half-model, to be tested at the NLR/HST or the ARA for engine integration. This model is equipped with extensive pressure plotting and calibrated through-flow-nacelles (TFN). Due to its modular structure contour modifications to reduce the engine interference are possible. For the propfan integration a powered version of this half model is used with pressure plotting on fuselage and pylon. The concept for determination of interference drag is discussed in chapter 6. Later on the halfmodel is equipped with a high-lift system for LS-configuration development in the Low-Speed Windtunnel (LSWT) in Bremen and High-Re checks in the F1 tunnel in Fauga. A turbo-powered simulator (TPS) will be installed then to check jet interference.

3. A 1:7 scale complete model for LS performance stability & control, and tail development for the DNW as well as for the HS tunnel S1 Modane for loads purposes and HS performance checkout.

The development of a laminar wing however is not possible with standard windtunnel testing only. It requests the implementation of new testing techniques for the windtunnel to get detail information of the boundary layer state and to enable an analysis of the stability phenomena. This must be supported by flight tests on the same geometry in order to establish a correlation, check the change of stability modes with Reynoldsnumber and develop design criteria.

The complete development concept to enable a trade-off of the different technologies is depicted in Fig. 11. The former VFW614-ATTAS aircraft (Fig. 12) was used as a flying test-bed with a laminar glove outboard of the pylon. Transition locations were measured by infra-red imaging and hot films and the pressure distribution was measured by means of a very fast PSI-system. A correlation was made possible by using a 1:2 scale half model tested in the DNW and the S1 where remote controlled flaps could be used to match the pressure distribution exactly with the flight test conditions. In addition a wake rake was installed to measure section drags. This was subject of the national research program ZKP-TLF I which was performed in close cooperation with the DLR and universities.

IV. Design of NLF-Airfoils

4.1 Design Method

The different modes of laminar-turbulent transition on a swept wing require different optimum pressure distributions to obtain laminar flow runs of the desired extent. Boundary layer profiles on a swept wing can be splitted into a profile in direction of the outer flow and a cross-flow profile which exhibits a maximum shear close to the wall (Fig. 13). In relation with these profiles there are three different modes of instability which may cause transition to turbulent flow, namely

- o the amplification of a plane disturbance wave in the main flow direction, which is called Tollmien-Schlichting instability (TSI)
- o the cross-flow instability (CFI)
- o the attachment line transition (ALT)

The transition location as a function of pressure distribution, Reynoldsnumber and sweep angle is quite different for the three modes and it is of utmost importance to predict the transition location most accurately and find a good compromise with respect to off-design cases. For the prediction of TSI efficient empirical criteria are available and for ALT the Poll-criterion seems to work also at high Re-numbers [19].

For cross-flow instability the only access is to use the stability theory for laminar boundary layers. The solutions of the Orr-Sommerfeld equation, which is a two-dimensional disturbance equation in direction of the disturbance wave front, are amplification ratios for disturbance waves of different wave length, frequencies and propagation direction (see Fig. 13). The integration of the amplification rates yields the amplitude ratio at each point of the airfoil. This is an exponential function e^N, where $N = \ln (A/Ao)$ is the factor to be determined by correlation of stability analysis and experiment. For the calculation of the N-factors the SALLY-Code was developped [20,21], which is valid for incompressible parallel flow without curvature effects.

By means of experimental investigation of the transition location for different modes, as it was done in the research program using the ATTAS aircraft, a correlation of N-factors for CFI and TSI can be determined as it is shown in Fig. 13. The result is a limiting band of N-factors which can be used for further optimization, provided the pressure distribution type is kept and the two modes are more or less decoupled.

TSI can be delayed by using a moderate continuous acceleration (see Fig. 7). The gradient must be increased with increasing Re-number. Cross-flow amplification can be kept small however with a sharp pressure drop at the leading-edge which causes a stronger growth of CF-waves, but downstream the crossflow becomes stable [22]. The required changes in pressure distribution to reduce CFI are quite small and difficult to achieve with an inverse code prescribing Cp = f(x), because it is important to have a high gradient dcp/ds along the arc length and this is a priori unknown. Hence the design is an iterative procedure which is illustrated in Fig. 14.

The pressure distribution of each design step is then calculated using a locally infinite swept wing analysis (LISWA) which utilizes a well-proven and reliable full-potential solver coupled with a semi-inverse boundary layer integral method simulating the wake curvature and thickness [23,24]. This code is used in the LISWA method by using the transformations for a swept, tapered wing. In addition the induced angle of attack is calculated from the complete singularity distribution of a lifting surface method. Both, lift and effective angle of attack at the nose, are prescribed then in the LISWA code. Normally this would be an ill-posed problem for a quasi 2D-solver. This is overcome by introducing a vortex which causes a curved flowfield. By applying this engineering method a quite accurate presentation of the leading-edge flow and pressure distribution is achieved, a prerequisite for the stability analysis.

4.2 Wing Glove Verification

The validation of such designs in the windtunnel and comparison with calculations is difficult as the surface quality must be extremely high and premature transition may occur due to roughnesses, steps, degree of turbulence and noise in the tunnel. The pressure hole itself may cause transition, hence imposing certain constraints on diameter and location of the holes in order to keep the downstream holes out of the turbulent wedge of the upstream holes. Some of these problems of the tests on the laminar glove (Fig. 12) are discussed in [25]. Additionally laminar separation bubbles at the beginning of the recompression may occur in the windtunnel which are not existing in flight. For performance predictions it is hence necessary to fix the transition some percent before the pressure minimum. Each testpoint should be checked by infra-red imaging in order to get the actual transition location.

As a typical result for the evaluation of transition locations during the flight tests may serve Fig. 15. At zero sideslip the transition is between 40% and 50% due to TSI. The wedges are stemming from artificial disturbances. At -3,5° sideslip (effective sweep increased) the typical wavy transition front due to CFI is visible. These locations were correlated with the N-factor envelopes calculated for the measured pressure distribution resulting in a limiting band of N_{CFI}-, N_{TSI}-factors, which can be used for the optimization of further designs more correlated to the aircraft project. The same procedure was repeated with the halfmodel in the S1 MA in order to correlate stability limits for a given pressure distribution for different Re-numbers.

V. Design and Verification of an NLF-wing

5.1 Basic airfoil design

Based on the experience of the research program a basic laminar airfoil was designed to match the design requirements of MPC 75 (Fig. 3). Originally a design Machnumber of 0.73 was requested as the UDF engine GE 38 under consideration at that time was short of thrust at higher Machnumbers. In case of a switch to a turbofan a higher Machnumber flexibility would be beneficial and this was the reason of a shift of the design point to M = 0.75 and a section lift of Cl = 0.4.

A 2D calculation for the design case and an off-design case (M = 0.7) is depicted in Fig. 16. The shock position is reasonably stable and the wave drag is kept low. At the cruise Re-number of ~ 20 Mio. a laminar bucket from CL = 0.25 to 0.6 was predicted, which is quite large. The lower surface distribution is nearly independent from Machnumber whereas the upper surface exhibits more pronounced suction peaks at the lower Machnumber thus reducing the upper limit of the bucket to CL = 0.3. A VC-flap will reduce the required angle of attack and enable a larger laminar bucket also in off-design.

The airfoil was tested in the TWB at the DLR at Brunswick at Re = $6 \cdot 10^6$. Fig. 17 shows a comparison of measurement and computation for fixed and free transition. The fixed transition drag levels are compared with the conventional transonic airfoil Va 2 which has a thickness of 12.93%. For comparibility the thickness effect was computed and subtracted. Even then the turbulent drag level of the laminar airfoil is competitive which gave rise to the thought to use such an airfoil even in the case when the laminarization would be discarded for the project.

5.2 Design and Verification of the first NLF-wings

5.2.1 High Speed Design

After verification in 2D a first NLF-wing was designed with the planform described in Fig. 4. After transposition of the airfoil design into a 3D design by means of the 3D direct-inverse method in [18] and the lofting of the basic NLF wing a conventional turbulent wing was designed as a competitor and gauge. This wing had a comparable thickness, but increased sweep (24,4° at the leading edge) and a $5m^2$ smaller wing area as it was assumed to have slats.

A comparison of the definition airfoils, Fig. 18, at 35% span shows some clear advantage for the laminar airfoil. Due to the longer acceleration distance the point of maximum thickness is shifted

rearward resulting in ~ 46% increased height of the rear spar. At same thickness and wing size this is worth 5% more fuel volume and 7% less wing weight due to the lighter flaps, spoiler structure and box weights.

In Fig. 19 the measured pressure distribution of both wings is shown in comparison to the calculation for fixed transition at 15% chord. The NLF wing exhibits a good isobar concept on the outboard wing and no adverse effect due to the steeper recompression. The body-juncture interference was not yet compensated correctly which results in the large suction peak at the root section. This gives an unfavourable large zone of turbulent flow on the inboard wing in the transition free case. The conventional wing shows a satisfactory design inboard whereas the isobar concept on the outboard wing needs some improvement.

Based on these initial design steps a design refinement was made in several aspects. First of all the trapezoidal wing planform had to be translated to a cranked one with 20° LE sweep as the Machnumber target was again shifted to Mec = 0.76 with the trend to even higher values and the decision to drop the propfan concept and use a modern wing mounted turbofan. With the corresponding telescopic MLG a cranked wing is inevitable.

Secondly the aspect ratio was reduced to 10 as a result of structural optimization and the need for increased root chord to accomodate the MLG.

Finally the wing area was increased to 85 m^2 as the MTOW increased to approximately 34 to and the fuel volume limited the max. stretch capability.

The scaled aerodynamic efficiency of both designs using a reference method is illustrated in Fig. 20. The conventional wing already represents a high-standard compared with current regional aircraft. The NLF wing exhibits higher efficiences at lower Machnumbers and is competitive up to M = 0.77 with 20° LE-sweep whereas at same sweep it envelopes the conventional wing. A prediction for the laminarization potential was derived by means of scaling the drag levels for transition free and fixed and a somewhat arbitrary correction to account for the separation bubble, which was visualized in the windtunnel and will be diminished in flight. The edge of the bucket was determined by using the SALLY-code for several wing stations. In Fig. 16 lines of const. maximum amplification at x/c = 56% chord are plotted with varying lift for upper and lower surface. The intersections of these lines with the limiting band from the flight tests determine the width of the laminar bucket ranging from CL = 0.25 to CL = 0.6 at M = 0.75. This was valid for a L.E. sweep of 17°. For 20° the inboard wing sections are already close to the limit and the upper limit decreases to 0.55. Beyond this sweep angle laminarity will be lost over a large extent of the wing span due to CFI. The improvement potential is ~ 13% which exceeds the first estimate. The resulting L/D-level is almost comparable to large widebody aircraft as the A340.

The scaled buffet boundaries are given in Fig. 21 with lines of required lift for the baseline aircraft and a fictitious maximum stretched version with 120 pax. It is shown that buffet limits yield sufficient stretch potential and the NLF wing is even somewhat better.

5.2.2 Low Speed Design

The baseline aircraft is defined without L.E.-device, but the trade-off is made whether a slat is useful for the baseline or as an add-on item later on. A wing without L.E.-device - especially with wing mounted engines - may have a critical stall behaviour which was experienced earlier with the VFW614 or the Fo100.

As the NLF wing cannot use a L.E.-device in any case special attention was paid to this field. The general arrangement in Fig. 22 shows two single slotted fowler flaps with a 30% chord on the outboard wing and a shroud line at 90% chord. The flap span is 80%. A first check of L.E.-stall-criteria has shown that the outboard wing stations close to the flap end are close to the boundary of prevailing L.E. stall where a short bubble exists with the potential risk of a bubble burst. In[26] different L.E.-modifications were investigated on NACA-6-series airfoils. These modifications were computed with different codes as to mention the Eppler-Code[27] and validated with the experimental results. For the NLF wing a L.E.-modification was designed thereafter with a combination of radius increase and camber at the outboard wing station 75% span. The result is also shown in Fig. 22 which should yield a sound distance to the boundary of L.E.-stall. This was checked in the Fl-windtunnel and found to be sufficient.

Despite the lower maximum lift for the clean configuration the NLF wing may have a similar lift with deflected flaps than the conventional wing due to the much thicker flap and more favourable flap pressure distribution (Fig. 22). For performance calculations L/D estimates for an MPC 75 with and without L.E.-device were derived (Fig. 23) from the High-Re-Test in Fauga and earlier reference aircraft. The very stringent field requirements can be fulfilled with both versions after having improved the maximum lift with the L.E. modification. In terms of approach speed the slatless wing would call for a much larger wing area thus penalizing the cruise configuration. Consequently the natural choice for a conventional wing seems to be a slat already for the baseline version. Operational aspects as to mention the very low angle-of-attack during flare-out with the risk for nose landing gear loss and dramatic lift-loss due to ice accretion support this decision.

5.2.3 Further operational aspects

5.2.3.1 Surface quality assessment

In order to check the feasibility of the NLF-design with todays surface tolerance catalogue and a CFRP wing box with integrated nose a flight test with the ATTAS was performed with different disturbances simulating steps and single protuberances as for example rivets. The result was encouraging[25] as only disturbances in the region of 5 to 20% chord resulted in measurable displacements of the transition location. Hence the installation of a cleaning device in the vicinity of the attachment line seemed to be uncritical.

The empirical relations for critical surface roughnesses reported by Holmes [28] and Braslow [29] were transposed to the MPC 75 and found to be in good agreement with the flight test. The resulting required tolerances (Fig. 24) are feasible with current manufacturing standards.

5.2.3.2 Decontamination of insect debris

A liquid anti-icing and cleaning element was tested on the flying test-bed. A cleaning success of more than 80% was achieved with a comparatively low amount of cleaning liquid. A transposition of these values to MPC 75 would result in ~10 kg for Take-off and Landing with an operating time of less than 5 min. As insect population growth is relevant only in a certain temperature and humidity environment the request for this cleaning device operative is only given in 1% of all annual flights according statistics. Hence it should be possible for the meteorologists at the airports to provide the pilot with the necessary information when to use the system as they already do with the anti-icing systems. Anti-icing cases however are much more probable (10% of all flights!).

To summarize chapter 5 one could say that generally NLF is ready to go, yet a lot of work is still to be done and the actual realization depends on the fuel price.

VI. Design Integration Aspects of a Propfan vs. a Turbofan

6.1 Propfan Integration

As propulsion system for MPC 75 a propfan engine was considered in an aft-mounted pusher configuration (Fig. 4). The design integration of these modern propellers requires a high interaction of various disciplines as the combined effects in terms of weight and drag may reduce the uninstalled propfan fuel savings significantly. The inherent problems of an aft-engine mounting lead to approximately 2-4% MWE increase already in a turbofan case. Installing a propfan means a weight penalty of ~10% due to the much higher propulsion system weight, the large pylon needed for blade tip clearance (~1,5 boundary-layer thickness) to the fuselage and runway thus resulting in large pitch-down thrust moments and trim loads [10]. The comprehensive design studies of MDC have even shown the necessity of a c.g. management system and additional pitch/yaw compensation systems [30].

Along with the overall configurational aspects challenging new tasks for the aerodynamicist remain to be solved which call for new measurement techniques and an intensive use of CFD methods as data of a flying reference aircraft or windtunnel measurements are not accessible. The most significant interference problems to be adressed are illustrated in Fig. 25 for Low-Speed and High-Speed. It is of utmost importance to know the flowfield (velocity and flow angularity), the disturbance pressure distribution on fuselage, and pylon with engine on/off, the interaction of engine sink effect on the wing wake, the boundary layer properties on the fuselage in order to

- o develop a contouring (area-ruling) of fuselage and nacelle
- o optimize pylon planform, thickness distribution and twist.
- o avoid unacceptable interference drags and losses of aircraft buffet limit due to premature pylon buffet
- o derive correct estimates for full-scale aircraft derivatives for longitudinal/lateral motion.
- o provide the engine manufacturer with the correct viscous flow field information in order to compute rotor fatigue and noise level.

A surface discretisation of a complete configuration with wing, body, fin, stabilizer, pylon and engine was worked out (Fig. 26) and calculated with the reknown panel code VSAERO for different powersettings in cruise and take-off configuration. A typical example of these calculations is the flowfield ahead of the front rotor disk (see Fig. 26). As the magnitude of the velocity deficit is most important for the noise level the wake velocities were computed via the quasi 2D method described earlier and superponed with the potential flow field in Fig. 27.

For the given pressure distribution a 3D boundary layer code was used to determine boundary layer thicknesses and the wall flow angles in order to determine blade tip clearance and the down-wash angle/gradient on the pylon which is more of 50% of its span inside the boundary layer.

A full potential code in finite-volume discretisation was used to determine the transonic effects of body, nacelle on the pylon (Fig. 28). The relative thickness of the pylon should not exceed 10-11% at the pylon-nacelle intersection. A chord extension together with a fillet should cure the problem but the structure/systems department are not satisfied with the cross-section as a lot of tubing/wiring must be incorporated and the asymmetric loads in case of a blade loss are dimensioning the pylon.

It was originally planned to report also a comparison of theory and experiment, but unfortunately the procurement of the propfan simulator, the implementation of the measurement technique, power supply and control unit, component balances took much longer than intended. So the results and the conclusion for the aerodynamic design will be subject of further publications. The problem areas to be addressed are depicted in Fig. 29. A 1:10 scale halfmodel will be used to determine the influence of the engine on the airframe and vice versa. At least 4 different model arrangements with different balances with variation of blade-setting and power-setting are necessary to determine interference drag. Pressure plotting on fuselage, pylon, nacelle and flowfield measurements with a rotating rake on the nacelle are planned additionally.

In the case of an integration in the aircraft, however, which may be derived when fuel prices increase again due to geopolitical reasons or fuel consumption limitations with respect to ecology, a flying test-bed like the UHB-demo of MDC is inevi-

table as there is a substantial lack of data in several fields which is not accessible for the european community. Hence such a demonstrator should be addressed in the framework of Brite/ Euram.

6.2 Turbo-Fan Installation

The under-wing turbofan installation on modern wide-body aircraft has been addressed in several publications [31,32,33] and is well understood in contrast to the propfan installation. However, recent examples of installing high-by-pass ratio engines on smaller aircraft like the B737-300[33] and the A320 have shown that considerable effort not only from the experimental side, but also from the CFD side was necessary to reduce installation drags to an acceptable level. With the advent of even higher by-pass ratios with the superfans or shrouded propfan (CRISP) this trend is enhanced.

In the case of MPC 75 a turbofan with by-pass-ratio of ~6 is foreseen at the moment including a long-duct nacelle with internal mixer and thrust reverser.

The typical integration aspects like runway-clearance in case of oleo collapse/flat tyre, flutter, engine disk burst, interference drag are aggravated when installing a long-duct nacelle on such a small aircraft. Taking into account growth potential up to 120 pax flap cut-outs, slat cut-outs will be inevitable thus evoking a lot of problems with maximum lift and stall control. Large MLG-fairings will be necessary which have to be designed with care in order to avoid excessive pressure drag.

A complete panel-model was worked out with nacelle, pylon and flap-track-fairings (Fig. 30) to study the mutual interference of the components for the conventional wing and the NLF wing. As the results in chapter 5 have shown, the NLF wing exhibited also very good turbulent drag levels and other advantages concerning fuel volume, system housing and wing weight, it was interesting to see the engine influence on this pressure distribution type also. An application of a new direct-inverse method modification on the wing sections in the presence of the engine can be performed now, which should reduce the negative effects on lift distribution and profile drag resulting in installation drags. A 2D-full potential solver is used to check the modifications during the iteration loop, whereas a final configuration will be calculated with a full 3D-Euler Code. An example for such a calculation is given in Fig. 31, where the unmodified NLF wing was computed with the RB 580 engine at cruise power setting. The isobar plot on the wing shows the unfavourable lift loss on the upper surface and the cross-section (ISO-Mach-plot) a quite unfavourable flowfield on the nacelle which tends to develop shocks at lower lifts.

VII. Economic Aspects and Conclusions

In the feasibility study and the beginning of the predevelopment phase the aforementioned technologies were investigated in detail partially supported by research programs. The evaluation was done by the project department based on DOC calculations taking into account the snowballing effects of the different technologies.

The comparison was done at a sector of 500 nm, which is a most probable route nowadays for a regional aircraft. Regarding the szenario in chapter I this may soon be leapfrogged by actual development of the market and the stretched version of MPC 75 already envisaged should cope with 2000 nm and even more. Hence the comparison at 500 nm with a fuel share of ~10% is somewhat conservative. The following results from this comparison

- o NLF technology with snowballing effects on engine and weight promises a 2% DOC saving (using the assumption of 13% L/D improvement) with an already inflated fuel price of 1$/gal. (Fig. 32).
- o propfan technology comes up with 10% weight increase and -16% blockfuel but 20% higher engine price resulting in even a DOC penalty of +1,3% (Fig. 32).

The conclusion was drawn that for the time being the extra effort for NLF technology as to mention liquid cleaning system, wing scrubbing over night, increased maintenance/repair due to undetachable leading edge and field limitations due to the lower lift capability without slats would be a difficult point to sell and even outbalance the improvement in DOC. As a consequence the NLF wing was replaced by a conventional wing. The airfoil type however, may be of some advantage and this is the reason why the development of this wing concept is pursued under the aspect of turbulent mode using a comparable planform than the conventional wing with higher sweep. One could think of a potential further development using one of the prototypes later on to check the laminarization potential using moderate suction at the nose and offering a HLFC version for the stretched variant.

As far as the propfan technology is concerned, the conclusion must be drawn, - and this was the worldwide common sense in 1989 - that its application would sell off only at much higher fuel prices than currently anticipated for the 1990's. In case of artificial fuel restrictions, which can be imagined from the ecologists side it offers an unmatched fuel-saving and might be revived sooner than expected.

VIII. Acknowledgements

The author likes to thank the staff of the aerodynamic design office for their valuable contribution as well as the departments for theoretical aerodynamics (potential flow, viscous flow) who contributed a variety of new codes and took part in the validation with experiments. Last but not least the tremendous work on the experimental side in windtunnel and flight must be appreciated as a keystone for the validation of the NLF wing, which was supported by the BMFT in the program ZKP-TLF I.

IX. References

1 J. Ott
Civil Aviation Must Tackle Major Challenges in 1990's
Aviation Week & Space Technology, Nov. 20, 1989

2 Interavia Airletter
No. 11, 752 - May 22, 1989-6

3 J. Ott
FAA Will Test Wayport Concept as Remedy to Airport Congestion,
Av. Week & Space Techn./Jan. 9, 1989

4 R. Schuil
The Wayport Concept
AIAA-paper 89-2057, August 1989

5 J.M. Swihart
Cost effective transportation and high technology.
Aeronautical Journal August/September 1986

6 B. Rek
Commuter Jets Gain Credibility
Interavia Aerospace Review 8/1989

7 P. Middleton
MPC Gears Up.
Flight International, 8 April 1989

8 E. Obert
The Aerodynamic Development of the Fokker 100
ICAS-88-1.6.2, Jerusalem/Israel

9 European Forum: The Evolution of Regional Aircraft Technologies and Certification.
Organized by DGLR, AAF, RAeS, April 6-7, 1989, Friedrichshafen

10 B. Fischer
Configurational Repercussions of New Technologies in the Design of a Regional Airliner
AIAA-paper 89-2022

11 R.L. James Jr., Dal V. Maddelon
The Drive for Energy Efficiency
Aerospace America, February 1984

12 G. Warwick
Jet-Star Smoothes the Way.
Flight International, 21 Sept. 1985

13 R.D. Wagner, D.W. Bartlett, F.S. Collier Jr.,
Laminar Flow - The Past, The Present and Prospects.
AIAA paper 89-0989

14 H. Körner, K.H. Horstmann, H. Köster, A. Quast and G. Redeker
Laminarization of Transport Aircraft Wings - A German View
AIAA-paper 87-0085

15 G. Redeker
Laminar Flow Wing
in 9

16 R. Hilbig and J. Szodruch
The Intelligent Wing
AIAA-paper 89-0534

17 E. Greff
Aerodynamic Design and Integration of a Variable Camber Wing for a New Generation Long/Medium Range Aircraft.
ICAS-88-2.2.4, Jerusalem/Israel

18 E. Greff and J. Mantel
An engineering approach to the inverse transonic wing design problem.
Intern. Conf. of Inverse Design Concepts in Engineer. Sci. (ICIDES), Oct. 84, Austin

19 D.I.A. Poll
Transition in the Infinite Swept Attachment Line Boundary Layer.
The Aeronautical Quarterly, Vol. 30, 1979, pp. 607-629

20 S.A. Orszag
Accurate Solution of the Orr-Sommerfeld Equation.
J. of Fluid Mech. 50 (1971), 689-703

21 A.J. Srokowsky and S.A. Orszag
SALLY LEVEL II USER'S GUIDE
Cosmic Programm # LAR-12556 (1979)

22 G. Redeker, K.H. Horstmann, H. Köster and A. Quast
Investigations on High Reynoldsnumber Laminar Flow Airfoils
J. Aircraft, Vol. 25, No. 7, July 1988

23 G. Dargel and P. Thiede
Viscous transonic airfoil flow simulation by an efficient viscous-inviscid interaction method. AIAA paper 87-0412, Jan. 1987

24 Terry Holst
Viscous Transonic Airfoil Workshop.
AIAA paper 87-1460, June 1987, Honolulu

25 U. Dreßler and R. Henke
Untersuchungen am Flugversuchträger ATTAS mit Laminarhandschuh und dessen 1:2 Großmodell im DNW und S1
DGLR Annual Meeting, Oct. 1989, Hamburg

26 J.A. Kelly
Effects of Modifications to the Leading-Edge Region on the Stalling Characteristics of the NACA 63-012 Airfoil Section
NACA TN 2228

27 Eppler, Somers
A Computer Program for the Design and Analysis of Low-Speed Airfoils
NASA T80 210, 1980

28 B.J. Holmes
Natural Laminar Flow Hit Smoother Air
Aerospace America/July 1985

29 A.L. Braslow and M.C. Fischer
Design Considerations for Application of Laminar Flow Control Systems to Transport Aircraft.
AGARD/FDP VKI Special Course on Aircraft Drag prediction and Reduction
May 20-23, 1985 Brussels, Belgium

30 P.A. Henne
MD-90 Transport Aircraft Design
AIAA-paper 89-2023

31 W.C. Swan, A. Sigalla
The Problem of Installing a Modern High Bypass Engine on a Twin Jet Transport Aircraft
AGARD CP-124, April 1973

32 M. Ehrmann, K.D. Klevenhusen, K. Rudolph, W. Burgsmüller
Computation of engine-airframe interference flows at subsonic and transonic speeds,
ICAS-paper No. 84-2.10.1, Toulouse 1984

33 E.N. Tinoco
Transonic CFD Applications at Boeing.
Transonic Symposium Theory, Application, and Experiment.
April 19-21, 1988, NASA Langley

X. Figures

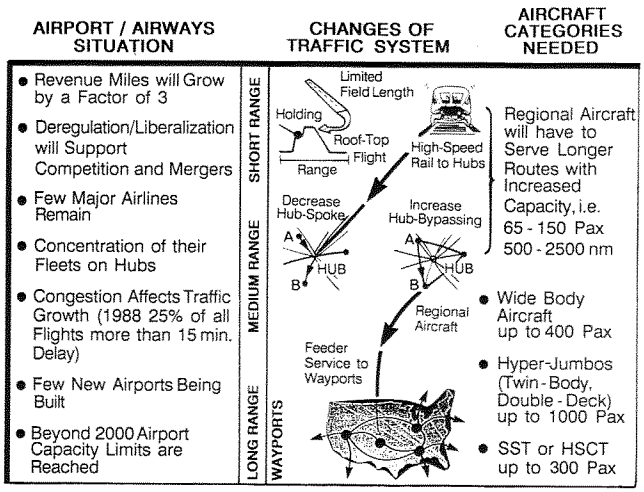

Fig. 1 Airline / Airways - Szenario 2008

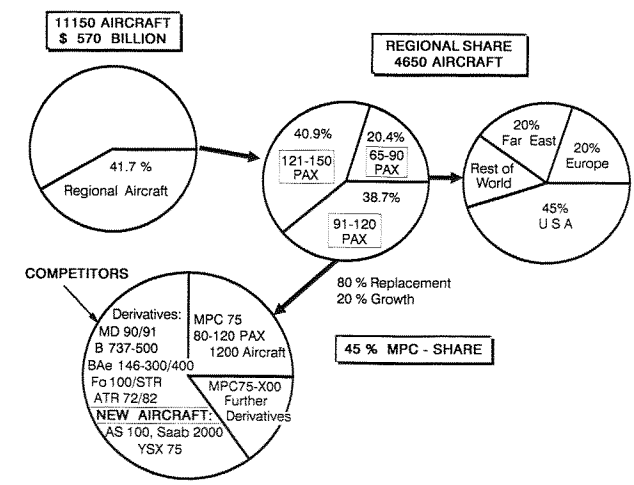

Fig. 2 Market Share of Regional Aircraft (1989-2008)

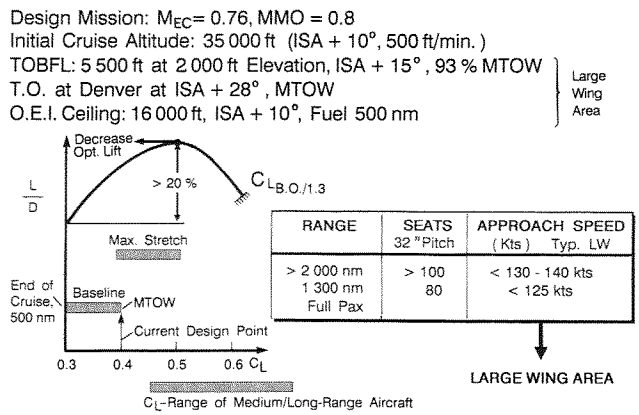

Fig. 3 Design Requirements Affecting Aerodynamic Design

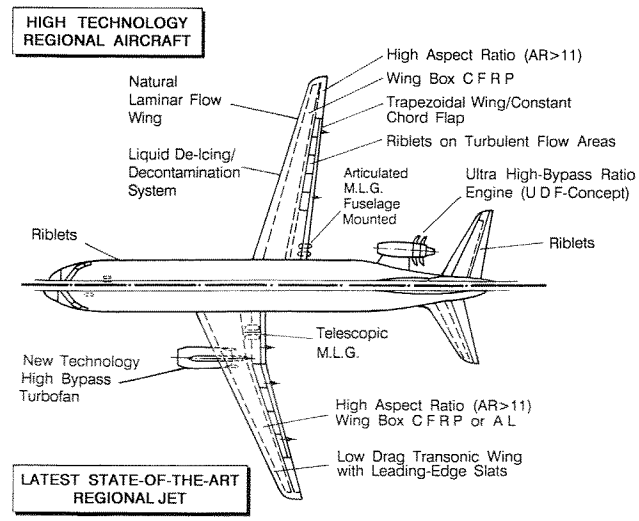

Fig. 4 Comparison of Basic Configurations

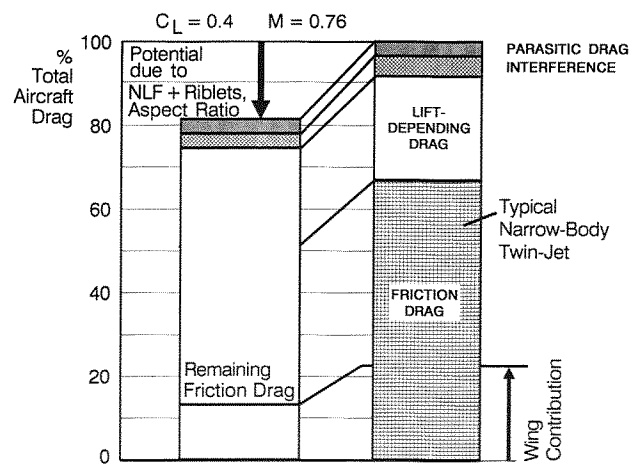

Fig. 5 Drag Breakdown in Cruise

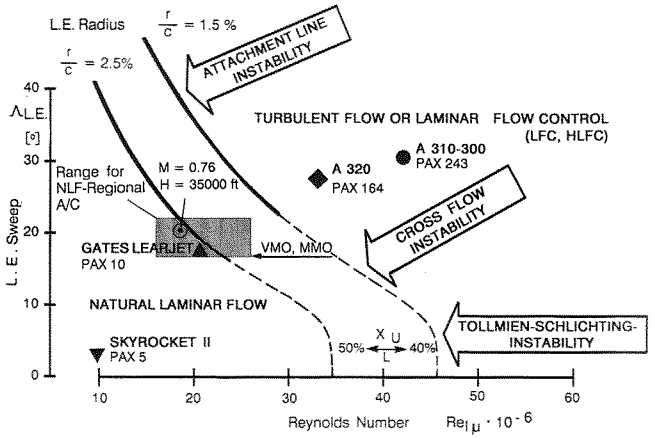

Fig. 6 Boundary for Swept Wing Laminarization

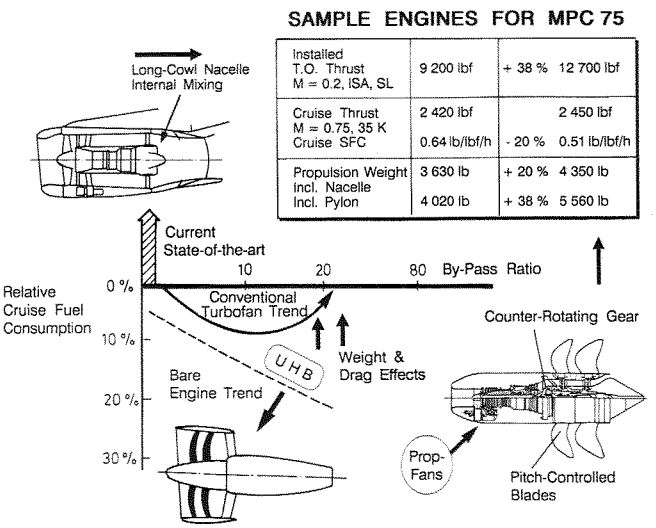

Fig. 9 Fuel Savings due to Engine Technology

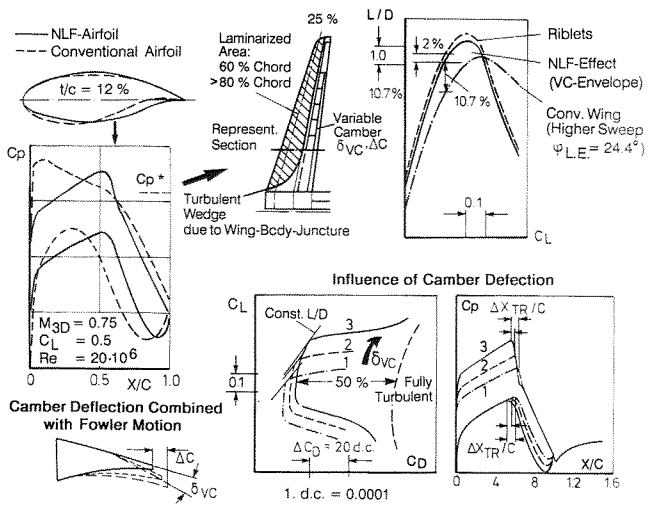

Fig. 7 Principle and Potential of NLF-Technology

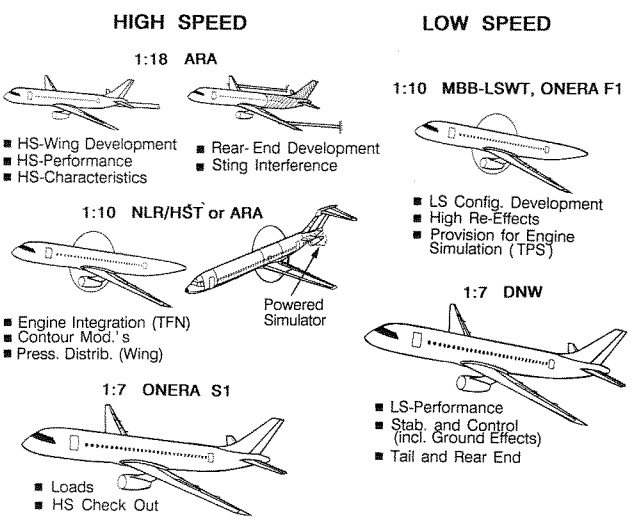

Fig. 10 Model and Wind Tunnel Strategy

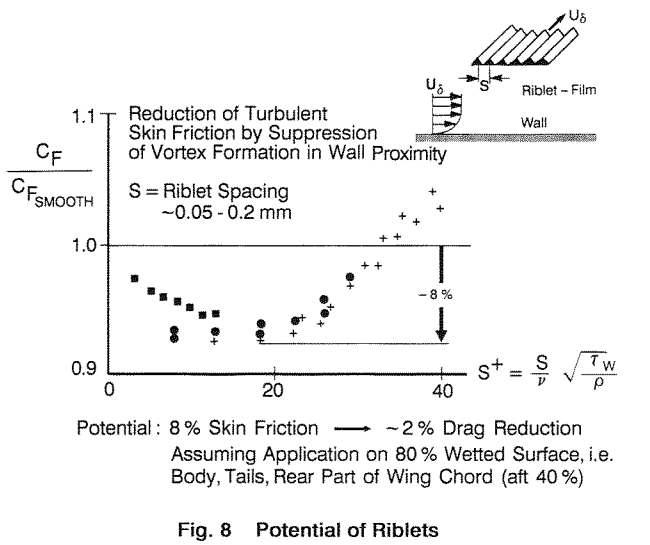

Potential: 8 % Skin Friction ⟶ ~2 % Drag Reduction
Assuming Application on 80 % Wetted Surface, i.e. Body, Tails, Rear Part of Wing Chord (aft 40 %)

Fig. 8 Potential of Riblets

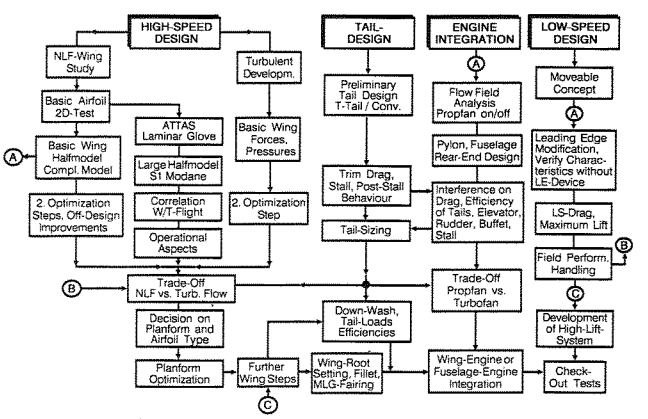

Fig. 11 Aerodynamic Development Concept

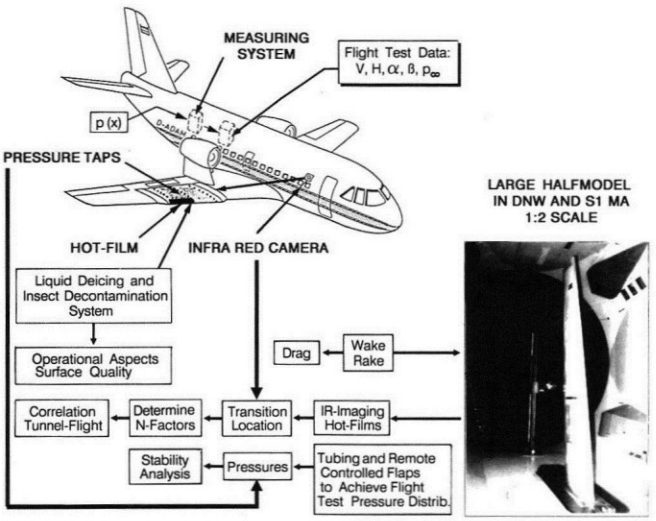

Fig. 12 NLF Technology Program

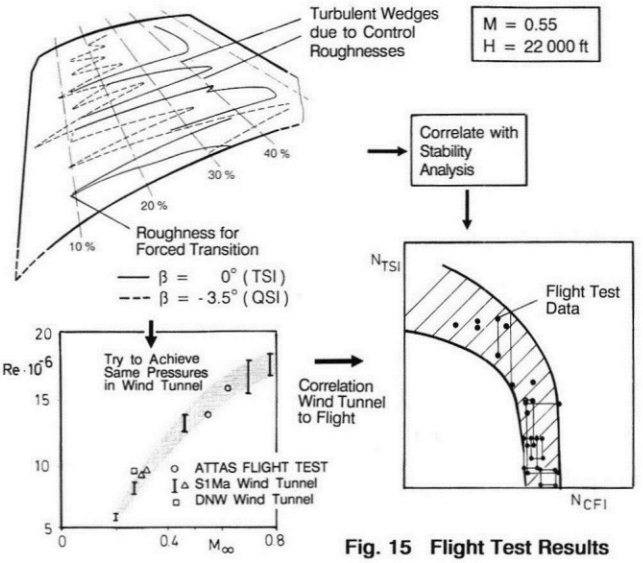

Fig. 15 Flight Test Results

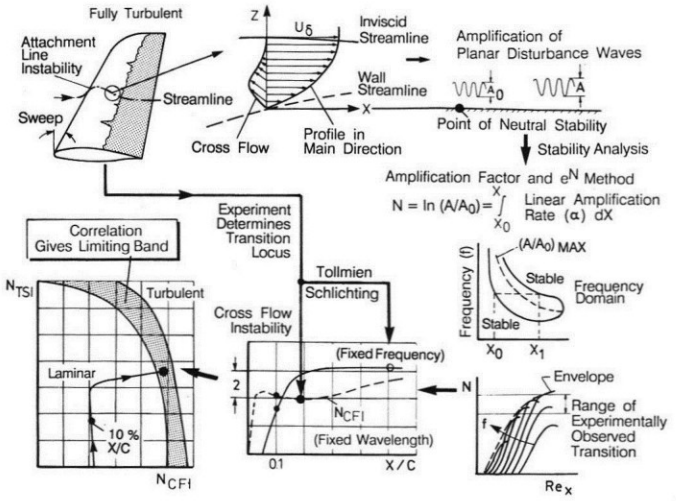

Fig. 13 Determination of Amplification-Exponents

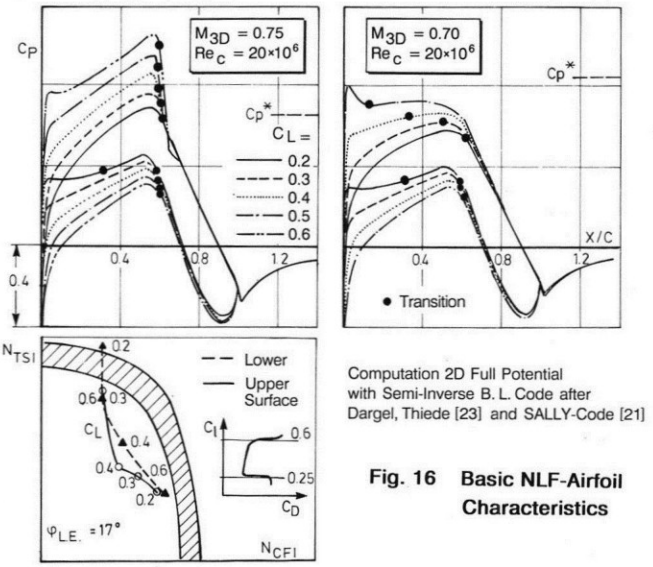

Computation 2D Full Potential with Semi-Inverse B. L. Code after Dargel, Thiede [23] and SALLY-Code [21]

Fig. 16 Basic NLF-Airfoil Characteristics

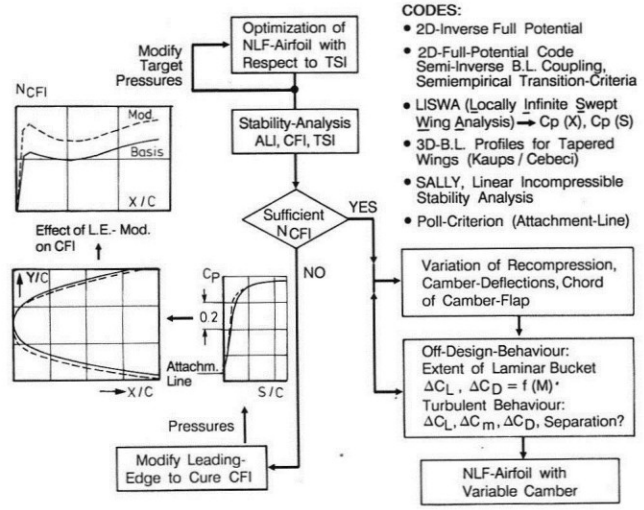

Fig. 14 Design of an NLF-Airfoil

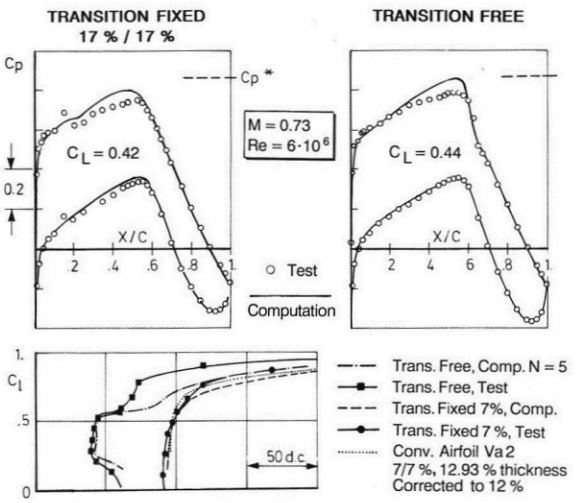

Fig. 17 Comparison of Experiment / Theory for NLF-Airfoil

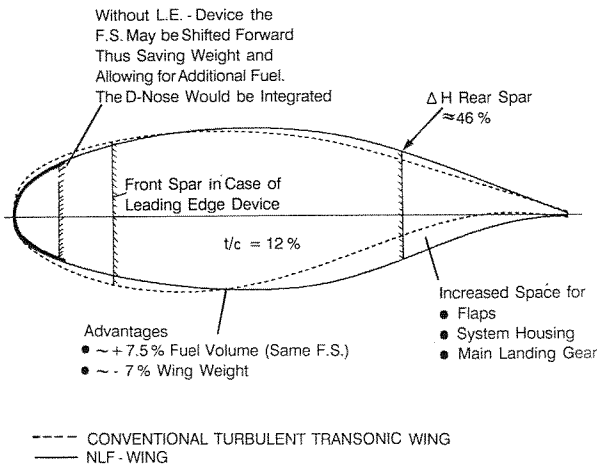

Fig. 18 Comparison of Typical Wing Sections

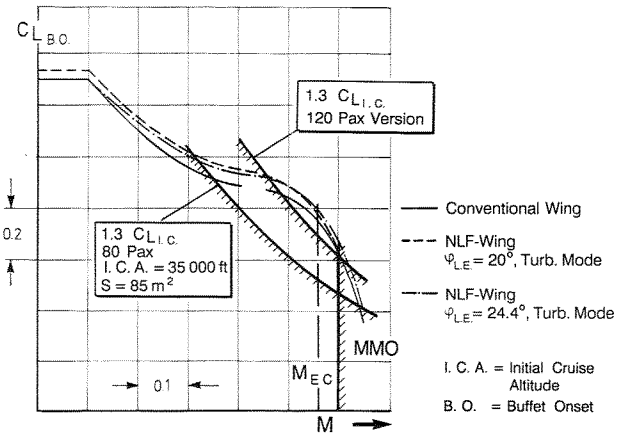

Fig. 21 Buffet Boundaries

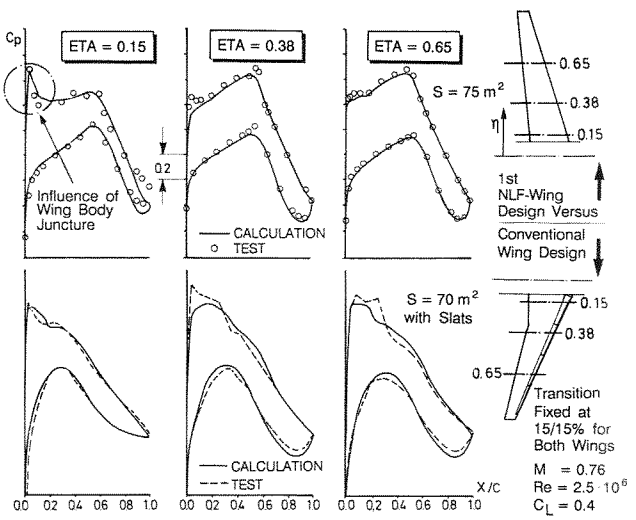

Fig. 19 Comparison of Spanwise Pressure Distribution

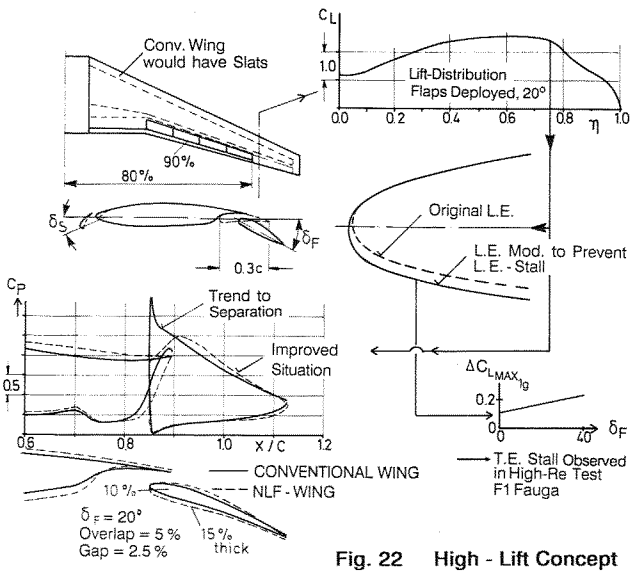

Fig. 22 High - Lift Concept

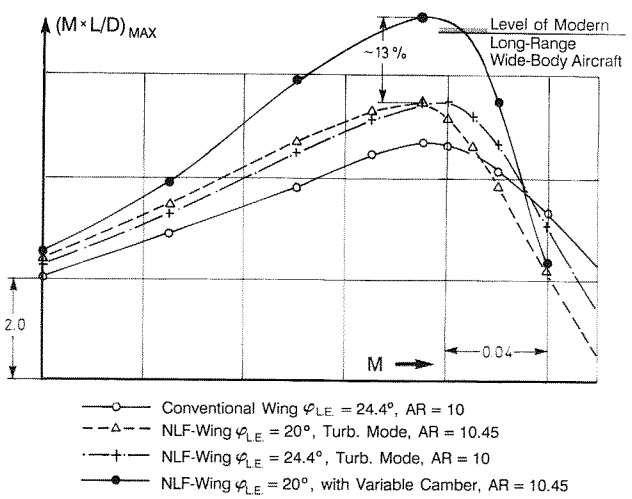

Fig. 20 Scaled Aerodynamic Efficiency $(M \times L/D)_{MAX}$

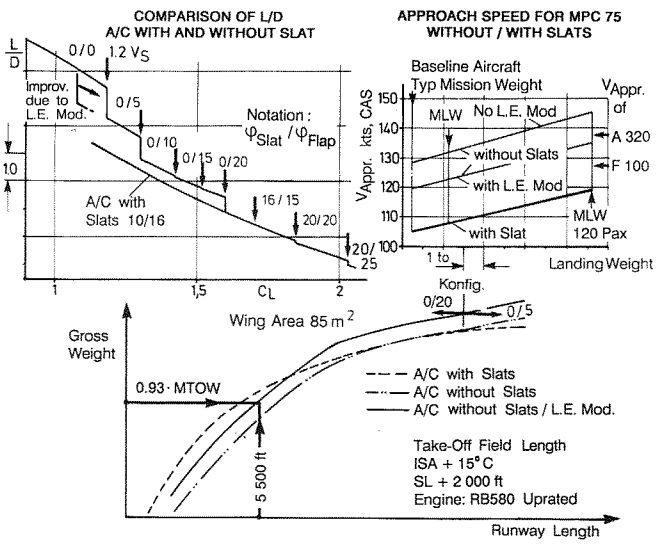

Fig. 23 Field Performance

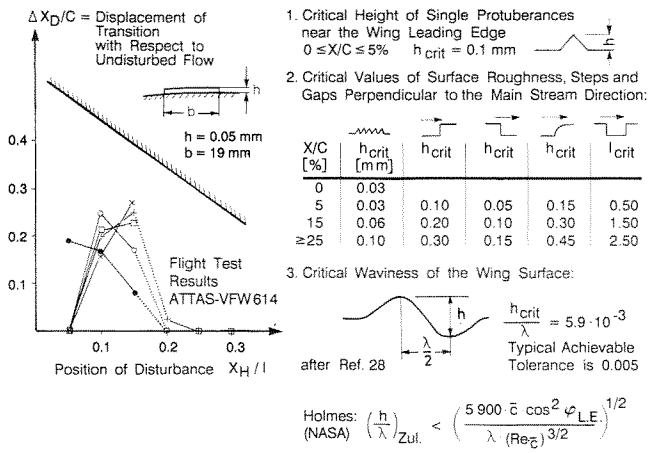

Fig. 24 Effects of Surface Quality on Transition

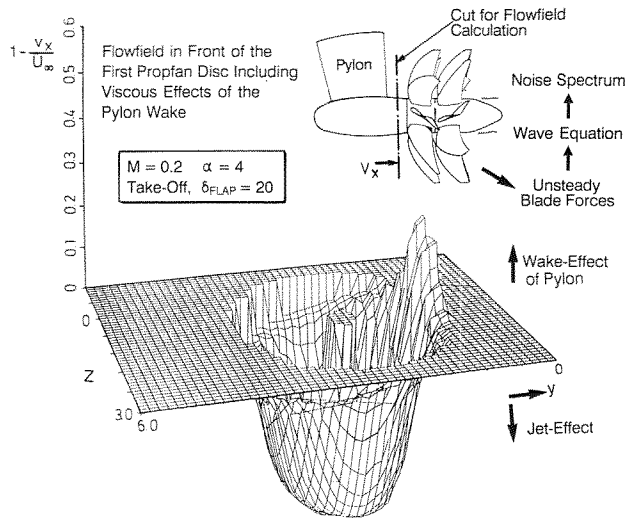

Fig. 27 Viscous Flowfield as Input for Noise Prediction

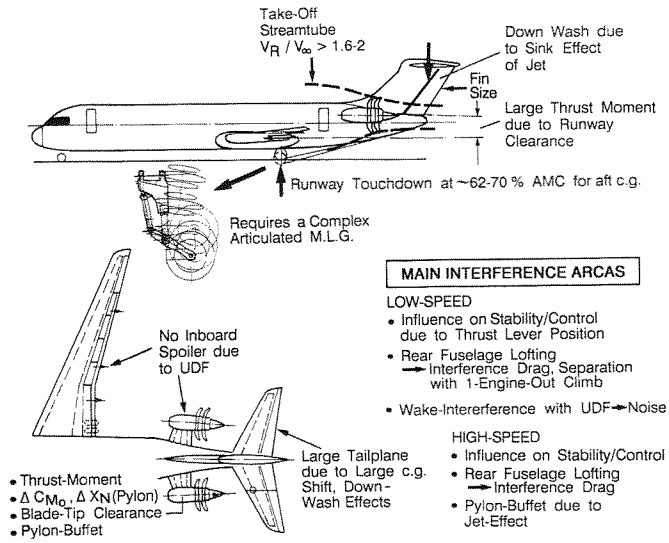

Fig. 25 Interference Problems with UDF-Propulson

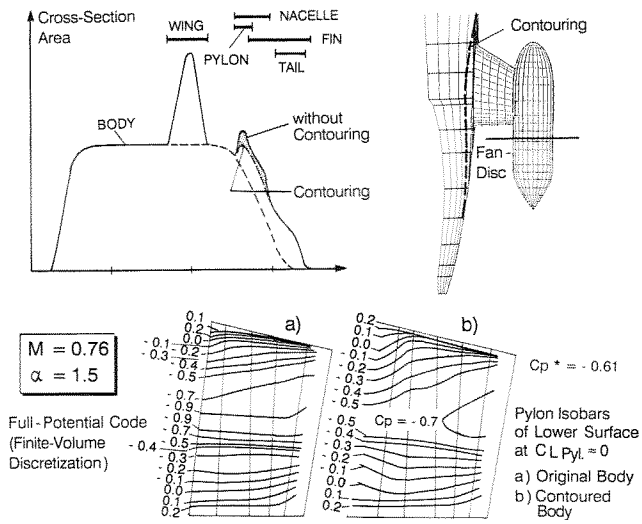

Fig. 28 Contouring of Fuselage

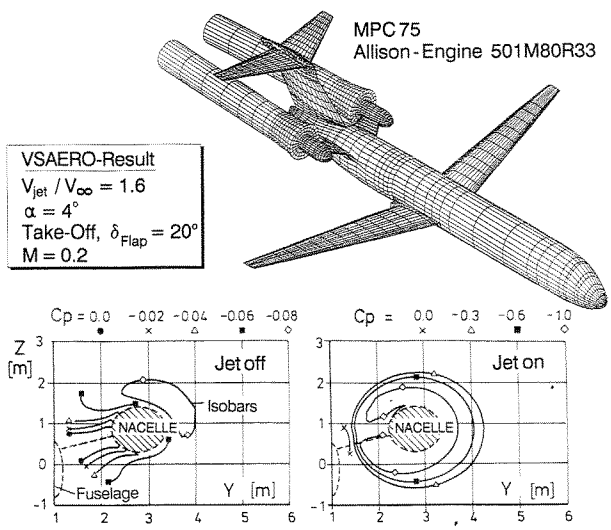

Fig. 26 U D F - Effects Low Speed

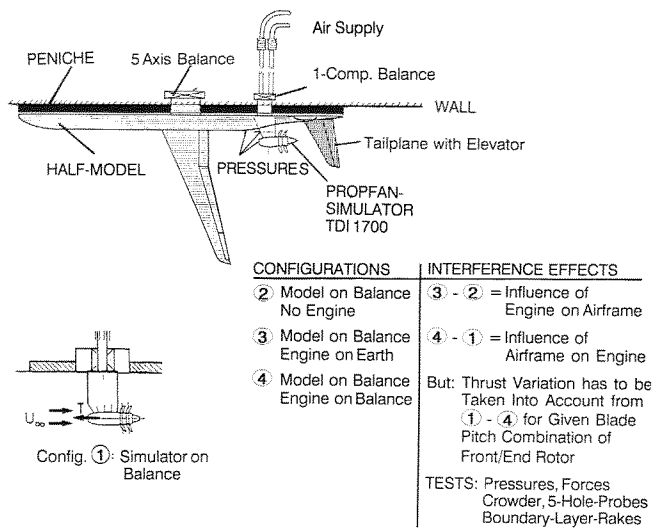

Fig. 29 Test-Setup for Engine Integration

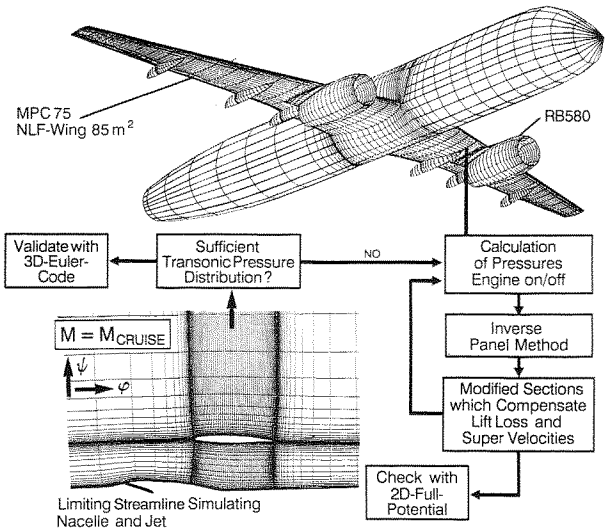

Fig. 30 Method for Minimization of Engine Interference

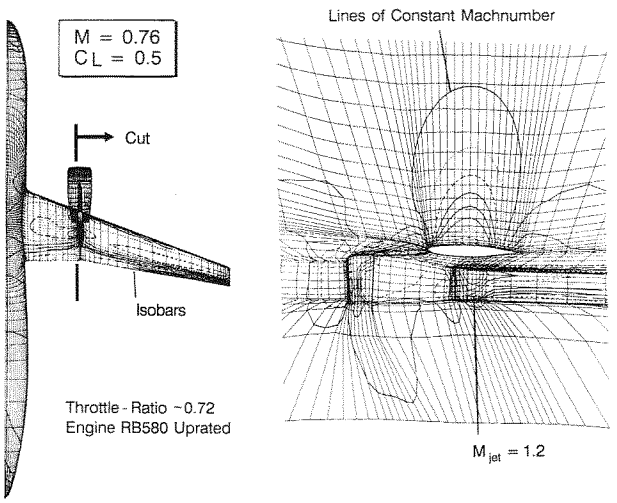

Fig. 31 Result of Euler-Code on Unmodified Wing

	LAMINAR WING (NLF) VERSUS TURBULENT WING	PROPFAN VERSUS STATE-OF-THE-ART TURBOFAN
	Change %	Change %
Manufacturers Weight Emply	- 1.0	+ 10.0
Total Fuel	- 11.7	- 17.0
Max. Take-Off Weight	- 2.0	+ 5.0
Thrust Required at Take-Off (M = 0.2)	- 2.0	+ 5.5
at Cruise (0.76)	- 13.0	+ 4.5
Blockfuel (Assuming 13 % Improvement)	- 11.7	- 16.0
Engine Price	- 2.6	+ 20.0
Aircraft Price	- 1.8	+ 7.0
Direct Operating Cost (500 n m) at Fuel Price of 1 $ / Gallon	- 2.0	+ 1.3

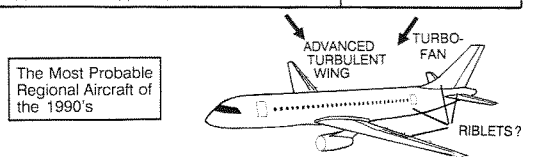

Fig. 32 Effect of New Technologies on DOC